Thermodynamics of vapor-liquid equilibria in aqueous solutions of acid gas-alkanolamine

Eduardo Buenrostro-González, Fernando García-Sánchez,* and Otilio Hernández-Garduza
Instituto Mexicano del Petróleo, Subdirección de Transformación Industrial-Gerencia de Investigación Aplicada de Procesos
Eje Central Lázaro Cárdenas 152, 07730 México, D.F., Mexico

Enrique Bazúa Rueda
Facultad de Química, Universidad Nacional Autónoma de México
04510 México, D.F., Mexico

Recibido el 14 de enero de 1998; aceptado el 23 de marzo de 1998

A thermodynamic model was developed for representing the solubility data of hydrogen sulfide (H_2S) and/or carbon dioxide (CO_2) in aqueous solutions of monoethanolamine (MEA), diethanolamine (DEA), diglycolamine (DGA), and methyldiethanolamine (MDEA). In order to determine the true compositions of all liquid-phase species, ionic and molecular, the model accounts for chemical equilibria in a rigorous fashion by using the nonstoichiometric formulation for nonideal solutions proposed by Smith and Missen. In this work, the system is assumed to be a solution formed of molecular (H_2S and/or CO_2) and ionic solutes in a mixture of two solvents (water and alkanolamine). The equilibrium properties of the ionic and nonionic species in aqueous-nonaqueous solvent mixtures were represented with the Electrolyte-NRTL excess Gibbs function which treats both long-range ion-ion interactions and local interactions between all liquid-phase species, while the vapor-phase was represented with the PRSV (Peng-Robinson-Stryjek-Vera) equation of state. Interaction parameters of the Electrolyte-NRTL equation were estimated upon the representation of vapor-liquid equilibrium data of water-alkanolamine and acid gas-water-alkanolamine systems. On the whole, good agreement was found between experimental and calculated partial pressures of H_2S and CO_2 for aqueous solutions of either one acid gas in MEA, DEA, DGA, and MDEA.

Keywords: Phase equilibria; chemical equilibria; equation of state; solution model

Se desarrolló un modelo termodinámico para representar los datos de solubilidad del ácido sulfhídrico (H_2S) y/o bióxido de carbono (CO_2) en soluciones acuosas de monoetanolamina (MEA), dietanolamina (DEA), diglicolamina (DGA) y metildietanolamina (MDEA). Con la finalidad de determinar las composiciones reales de todas las especies en la fase líquida, iónicas y moleculares, el modelo considera en forma rigurosa el cálculo del equilibrio químico a partir de la formulación no estequiométrica para soluciones no ideales propuesto por Smith y Missen. En este trabajo se considera que el sistema bajo estudio es una solución formada de solutos iónicos y moleculares (H_2S y/o CO_2) en una mezcla de dos disolventes (agua y alcanolamina). Las propiedades de equilibrio de las especies iónicas y moleculares en mezclas de disolventes acuosos-no acuosos fueron representadas con la función de Gibbs de exceso NRTL-electrolitos, la cual trata las interacciones ion-ion de largo alcance y las interacciones locales entre todas las especies de la fase líquida, mientras que la fase vapor fue representada con la ecuación de estado PRSV (Peng-Robinson-Stryjek-Vera). Los parámetros de interacción del modelo NRTL-electrolitos fueron estimados a partir de la representación de datos de equilibrio líquido-vapor de los sistemas agua-alcanolamina y gas ácido-agua-alcanolamina. En general se obtuvo buen acuerdo entre las presiones parciales experimentales y calculadas de H_2S y CO_2 para las soluciones acuosas de un gas ácido en MEA, DEA, DGA y MDEA.

Descriptores: Equilibrio de fases; equilibrio químico; ecuación de estado; modelo de solución

PACS: 05.70.-a; 05.70.Ce; 64.70.-p; 64.70.Fx

1. Introduction

Acid gases such as hydrogen sulfide and carbon dioxide existing in natural gas and refinery process streams, among others, are usually removed using aqueous solutions of alkanolamines in absorption/stripping operations. Hydrogen sulfide, due mainly to its high toxicity and corrosive effects, must be removed completely from the source gases to avoid catalyst poisoning in refinery operations, while carbon dioxide is removed from natural gas because it acts as a diluent, increasing transportation costs and reducing the energy value per unit of gas. In addition, carbon dioxide is separated from reformer product gas in the production of ammonia to avoid poisons synthesis catalyst in the ammonia converter.

Actually, there is a variety of processes for removal of acid gases from the source gas streams known as gas-treating processes. In particular, the process of absorption/stripping is one of the most widely used in the gas industry. This process is characterized as mass transfer enhanced by chemical reaction in which the presence of an alkanolamine enhances the solubility of an acid gas in the aqueous phase at a constant value of the equilibrium partial pressure. Thus, based on a set of chemical reactions with the acid gases, the use of aqueous solutions of alkanolamines, increases the absorption in these processes.

The absorption/stripping operations are applied mainly for the purification of sour gas streams, which have low and

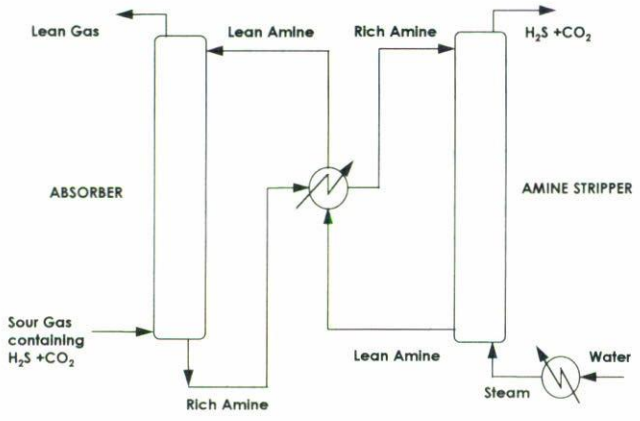

FIGURE 1. Simplified flow schematic of a typical gas treating operation which employs an aqueous alkanolamine solution in absorption/stripping.

moderate concentrations in acid gases (1–40% mol). Figure 1 shows a simplified gas treating process that employs an aqueous alkanolamine solution in absorption/stripping operation. In this process, a sour gas containing H_2S and/or CO_2 is introduced at the bottom of an absorber where it rises and contacts in countercurrent with an aqueous solution of alkanolamine that is introduced at the top of the absorber at about 40°C. The pressure of the absorber varies depending upon the sour gas stream being treated. The aqueous alkanolamine solution selectively absorbs the acid components from the sour gas to produce a "sweet" gas stream. The alkanolamine solution rich in absorbed acid gases is pumped from the bottom of the absorber through heat exchangers where its temperature is raised. The amine solution is then introduced at the top of a stripper where it countercurrently steam at a reduced pressure and at temperature of about 120°C. The steam produced in a reboiler, provides the energy necessary to reverse the reactions of the acid gases with alkanolamine, increasing the acid gas partial pressure and, simultaneously, stripping the acid gases from the solution. The lean alkanolamine solution is then pumped through a heat exchanger, where it is cooled and reintroduced at the top of the absorber.

Alkanolamines are characterized as containing both hydroxyl groups and amino groups in their molecular structure. The hydroxyl groups of the alkanolamines allow reducing the vapor pressure and increasing water solubility while the amino groups provide the necessary alkalinity in the aqueous solution to react with the acid gases [1]. Currently, amines of interest in the gas industry include the monoethanolamine (MEA), diethanolamine (DEA), diglycolamine (DGA), methyldiethanolamine (MDEA), and diisopropylamine (DIPA). Aqueous solutions of (MEA) have been extensively used due to their high reactivity as well as the low cost of solvent and low solubility of hydrocarbons; however, the loading capacity of MEA solutions is lower than that of MDEA solutions due, mainly, to the formation of a rather stable carbamate. MDEA, on the contrary, has a higher loading capacity and low heat of reaction with the acid gases leading with this to lower requirements for regeneration; however, due to the low reaction of CO_2 with tertiary amines, the use of MDEA solutions is limited. Therefore, it seems that mixtures of primary (MEA) and tertiary (MDEA) amines, can be an alternative to enhance the loading capacity and the absorption rate of CO_2, bringing an improvement in absorption and in saving energy requirements (see Refs. 2 and 3).

Thus, design of gas treating absorption/stripping systems by the equilibrium stage approach requires a correct knowledge of the vapor-liquid equilibria behavior of the aqueous acid gas-alkanolamine system. That is, the equilibrium solubility of the acid gases in aqueous alkanoamine solutions allows to determine the minimum quantity of solution to treat a given sour gas, and to determine the maximum concentrations of the acid gases which can be left in the regenerated solution to meet the gas specifications of the product. Fortunately, there exists a large body of vapor-liquid equilibrium data for aqueous acid gas-alkanolamine systems reported in the literature; however, due to that most of these data were measured at high acid gas loading, only a little quantity of them corresponds to the low acid gas pressure range where it is most important because in this range, the vapor-liquid equilibria determines the limitation of the sweet gas purity. Consequently, an efficient and thermodynamically rigorous model is needed to represent the experimental data so that it can be confidently used to interpolate between and extrapolate beyond the available data, which results in the reduction of experimental effort required to characterize the vapor-liquid equilibria behavior of systems for which no data have been reported.

In this context, the research group of the Thermophysics laboratory of the Mexican Petroleum Institute has carried out a systematic study over the past 15 years to develop efficient natural gas treating processes, which involved the search of new solvents to improve the selectivity, absorption capacity, and low energy requirements. However, because the proper selection of a solvent for the treating of a given sour gas is difficult and requires of the evaluation of several thermodynamic properties as well as the knowledge of the vapor-liquid equilibria behavior of the systems. Since then, this group has measured and reported solubility data of H_2S, CO_2, and methane in pure physical (N-methylpyrrolidone, sulfolane, and propylene carbonate) solvents and mixed physical and chemical (MEA and DEA) solvents (see Refs. 4–10). Typically, the solubility data were measured in the temperature range from 25 to 100°C. Conclusions derived of this study showed that the blend of N-methylpyrrolidone with DEA presented a larger absorption capacity for both acid gases than those aqueous diethanolamine solutions used traditionally in natural gas treating. More recently, this group has undertaken a study concerning measurements of vapor-liquid equilibria of H_2S and CO_2 in both aqueous and nonaqueous alkanolamines (DEA and MDEA) solutions with and without physical solvent (N-methylpyrrolidone).

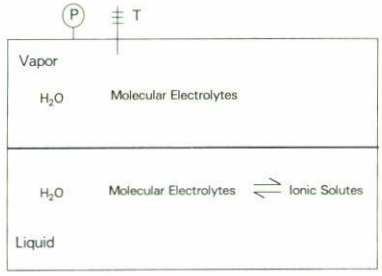

FIGURE 2. Phase and chemical equilibria in a closed weak electrolyte system.

Mixed amine systems have become widely used during the past decade or so, due mainly to their considerable commercial importance; however, only the model of Deshmukh and Mather [11] and the Electrolyte-NRTL model of Chen and Evans [12] have been extended to systems of mixed amines by Chakravarty [13] and by Austgen *et al.* [14, 15], respectively.

In this work, we have chosen the Austgen *et al.*'s implementation of the Electrolyte-NRTL model of Chen and Evans to represent the vapor-liquid equilibria in acid gas-alkanolamine-water systems. This thermodynamic model, although somewhat more complex than that of Deshmukh and Mather model, accounts for chemical equilibria in a rigorous manner to determine the true compositions of all liquid-phase species, ionic and molecular; the system being assumed to be a solution formed of molecular (H_2S and/or CO_2) and ionic solutes in a mixture of two solvents (water and alkanolamine).

The validity of the representation will be tested against experimental results while the extension of the model to correlate and predict the solubility of acid gases in mixed alkanolamine solutions will be presented in a forthcoming paper.

2. Thermodynamic model

As mentioned above, acid gases and alkanolamines are weak electrolytes which are partially dissociate in the aqueous phase to form a complex mixture of nonvolatile or moderately volatile solvent species (water and alkanolamine), high volatile molecular species (H_2S and/or CO_2), and nonvolatile ionic species. Figure 2 illustrates thc phase and chemical equilibria of a weak electrolyte system such as the acid gas-alkanolamine-water system. In a closed system, at constant temperature and pressure, the phase equilibria governs the distribution of electrolytes and molecular species between the liquid and vapor phases, while chemical reactions are carried out in the liquid phase between acid gases and alkanolamines to produce a number of ionic species. As shown in Fig. 2, phase and chemical equilibria are highly coupled in this system so that the degree of dissociation of the weak electrolytes in the liquid phase is influenced by the partial pressure of an acid gas in the vapor phase and vice versa. Hence, representation of the vapor-liquid equilibria behavior of acid gas-alkanolamine-water systems is complicated due to the large number of chemical reactions that occur in this system. On this basis, it is clear that representation of phase equilibria for such systems requires that both phase and chemical equilibria be rigorously accounted for.

2.1. Chemical equilibria

In the aqueous phase, the dissociation of the acid gases and alkanolamines can be expressed according to the following reactions [16]:

(ionization of water)

$$2H_2O \leftrightarrow H_3O^+ + OH^- \tag{1}$$

(dissociation of hydrogen sulfide)

$$H_2O + H_2S \leftrightarrow H_3O^+ + HS^- \tag{2}$$

(dissociation of bisulfide)

$$H_2O + HS^- \leftrightarrow H_3O^+ + S^= \tag{3}$$

(dissociation of carbon dioxide)

$$2H_2O + CO_2 \leftrightarrow H_3O^+ + HCO_3^- \tag{4}$$

(dissociation of bicarbonate)

$$H_2O + HCO_3^- \leftrightarrow H_3O^+ + CO_3^= \tag{5}$$

(dissociation of protonated alkanolamine)

$$H_2O + RR'R''NH^+ \leftrightarrow H_3O^+ + RR'R''N \tag{6}$$

where the term $RR'R''N$ denotes the chemical formula of the alkanolamine and R represents an alkyl group, alkanol group, or hydrogen. It is worth noting that reactions (2)–(6) are proton transfer reactions so that they occur very rapidly and are often assumed instantaneous with respect to mass transfer. It is well-known that primary and secondary amines react directly with CO_2 to form stable carbamates; however, as suggested by Austgen *et al.* [14], we consider the following reversion of carbamate to bicarbonate instead of the direct formation of carbamate,

(carbamate reversion to bicarbonate)

$$RNHCOO^- + H_2O \leftrightarrow RNH_2 + HCO_3^- \tag{7}$$

On the contrary, tertiary amines having no hydrogen on the amino group available for extraction, are unable to react with CO_2 to form carbamates.

Molecular electrolytes react or dissociate in the liquid phase to produce ionic species to an extent of R independent reactions governed by chemical equilibria according to the following expression:

$$\sum_{i=1}^{N} \nu_{ij}\mu_i = \sum_{i=1}^{N} \nu_{ij}\mu_i^\circ + RT \sum_{i=1}^{N} \nu_{ij} \ln a_i = 0, \qquad j = 1, \ldots, R \tag{8}$$

TABLE I. Temperature dependence of equilibrium constants for reactions given by Eqs. (1)–(7) and Henry's constants for H_2S and CO_2[a].

Equation number	Component	C_1	C_2	C_3	C_4	Temperature range (°C)
		Equilibrium constants: $\ln K = C_1 + C_2/T + C_3 \ln T + C_4 T$				
1		132.899	−13445.90	−22.4773	0.0	0–225
2		214.582	−12995.40	−33.5471	0.0	0–150
3		−32.000	−3338.00	0.0	0.0	14–70
4		231.465	−12092.10	−36.7816	0.0	0–225
5		216.049	−12431.70	−35.4819	0.0	0–225
6	MEA	2.1211	−8189.38	0.0	−0.007484	0–50
6	DEA	−6.7936	−5927.65	0.0	0.0	0–50
6	MDEA	−9.4165	−4234.98	0.0	0.0	25–60
6	DGA[b]	1.6957	−8431.65	0.0	−0.005037	
7	MEA[c]	3.29243	−3805.34	0.0	0.0	25–120
7	DEA[c]	3.28074	−2948.87	0.0	0.0	25–120
7	DGA[c]	8.84892	−5198.3	0.0	0.0	25–100
		Henry's constants: $\ln H^{P^\circ} = C_1 + C_2/T + C_3 \ln T + C_4 T$				
2	H_2S	358.138	−13236.8	−55.05510	0.059565	0–150
4	CO_2	170.7126	−8477.711	−21.95743	0.005781	0–100

[a] Austgen *et al.* [14, 15] [b] Dingman *et al.* [31] [c] Estimated from reported VLE data

where a_i, ν_i, and μ_i are, respectively, the activity, the stoichiometric coefficient, and the chemical potential of species i. In terms of mole fractions, x_i, and activity coefficients, γ_i, Eq. (8) can be written as

$$K_j = \prod_{i=1}^{N} (x_i \gamma_i)^{\nu_{ij}} = \exp\left(-\frac{1}{RT}\sum_{i=1}^{N} \nu_{ij}\mu_i^\circ\right) \qquad j = 1, \ldots, R \quad (9)$$

Eq. (9) relates the equilibrium constant, K_j, of reaction j to the N values of the reference state chemical potentials, μ_i°. For reactions given by Eqs. (1)–(7), the temperature dependence of the equilibrium constants, K, are represented by

$$\ln K = C_1 + C_2/T + C_3 \ln T + C_4 T, \quad (10)$$

where coefficients C_1–C_4 for all reactions considered are given in Table I.

2.2. Phase equilibria

Phase equilibria governs the distribution of molecular species between the liquid and vapor phases, $\hat{f}_i^V = \hat{f}_i^L$, where $\hat{f}_i$ is the fugacity of component i in the mixture and superscripts V and L stand for vapor the and liquid phases, respectively. For molecular solutes H_2S and CO_2, Henry's constants represent the reference-state fugacities expressed as follows:

$$y_i \hat{\phi}_i P = x_i \gamma_i^* H_i^{P^\circ} \exp\left[\frac{v_i^\infty (P - P_i^\circ)}{RT}\right], \qquad i = H_2S,\ CO_2, \quad (11)$$

where $H_i^{P^\circ}$ and v_i^∞ are, respectively, the Henry's constant and partial molar volume at infinite dilution for molecular solute i in pure water at the system temperature and at the vapor pressure of water. Temperature dependence of Henry's constants were estimated by the same functional form given by Eq. (10). Coefficients C_1–C_4 for H_2S and CO_2 Henry's constants are also given in Table I. Partial molar volumes of H_2S and CO_2 at infinity dilution in water were estimated by the correlation of Brelvi and O'Connell [17],

$$v_1^\infty = (1 - C_{12}^\circ) K_2^\circ RT, \quad 1 = H_2S, CO_2; \quad 2 = H_2O, \quad (12)$$

where coefficients C_{12}° and K_2° are estimated by the following relations:

$$\ln\left[-C_{12}^\circ \left(\frac{v_2^*}{v_1^*}\right)^{0.62}\right] = \begin{cases} -2.4467 + 2.12074\,\tilde{\rho} \\ \qquad \text{if } 2 \le \tilde{\rho} \le 2.785 \\ 3.02214 + 1.87085\,\tilde{\rho} \\ \qquad +0.71955\,\tilde{\rho}^2 \\ \qquad \text{if } 2.785 < \tilde{\rho} \le 3.2 \end{cases} \quad (13)$$

$$\ln\left[1 + \frac{1}{\rho K_2^\circ RT}\right] = -0.42704(\tilde{\rho} - 1) + 2.089(\tilde{\rho} - 1)^2 - 0.42367(\tilde{\rho} - 1)^3 \quad (14)$$

TABLE II. Temperature dependence of pure component vapor pressures of water and alkanolamines[a].

Component	D_1	D_2	D_3	D_4	D_5	D_6	D_7	Temperature range (°C)
Vapor pressures: $\ln P^\circ = D_1 + D_2/(T + D_3) + D_T + D_5 \ln T + D_6 T^{D_7}$								
H_2O	72.55	−7206.7	0.0	0.0	−7.1385	4.0460×10^{-6}	2	0–374
MEA	172.78	−13492.0	0.0	0.0	−21.914	1.3779×10^{-5}	2	10–365
DEA	286.01	−20360.0	0.0	0.0	−40.422	3.2378×10^{-2}	1	28–269
MDEA[b]	26.137	−7588.5	0.0	0.0	0.0	0.0	0	120–240
DGA[c]	20.86	−3314.83	0.0	0.0	0.0	0.0	0	

[a] Daubert and Danner [32] [b] Daubert and Hutchinson [33] [c] Austgen [34]

TABLE III. Pure component properties of water, acid gases, and alkanolamines.

Component	MW	T_c (K)	P_c (kPa)	V_c ($m^3 kmol^{-1}$)	Z_{RA}	w	κ_1
H_2S[a]	34.07	373.2	8926.9	0.0986		0.100	0.07149[d]
CO_2[a]	44.01	304.2	7376.5	0.0939		0.225	0.04285[e]
H_2O[a]	18.02	647.3	22090.0	0.0568	0.2338	0.344	−0.06635[e]
MEA[b]	61.08	638.0	6870.0	0.2250	0.2488	0.797	−0.28351[d]
DEA[b]	105.14	715.0	3270.0	0.3490	0.2527	1.046	−0.28351[d]
MDEA[c]	119.16	677.8	3876.1	0.3932	0.2522	1.242	−1.09940[f]
DGA[c]	105.14	674.6	4354.9	0.3270	0.2540	1.046	−0.51278[d]

[a] Reid *et al.* [35] [b] Daubert and Danner [32] [c] Austgen [34] [d] Estimated in this work
[e] Taken from Stryjek and Vera [21] [f] Taken from Carroll *et al.* [36]

In these equations, $\tilde{\rho} = \rho v_2^*$, where ρ and v_2^* are the molar density and characteristic volume of water which was set equal to 0.0464 $m^3 Kmol^{-1}$, while characteristic volumes, v_1^*, for H_2S and CO_2 were fixed at 0.0939 and 0.0887 $m^3 Kmol^{-1}$, respectively.

Vapor-liquid equilibria for the solvent species, water and alkanolamine, are given by,

$$y_s \hat{\phi}_s P = x_s \gamma_s P_s^\circ \hat{\phi}_s^\circ \exp\left[\frac{v_s(P - P_s^\circ)}{RT}\right], \qquad (15)$$

v_s being the molar volume of the pure solvent at the system temperature and saturation pressure. The temperature dependence of pure-component vapor pressures is represented by the following function,

$$\ln P^\circ = D_1 + \frac{D_2}{D_3 + T} + D_4 T + D_5 \ln T + D_6 T^{D_7}, \qquad (16)$$

where coefficients D_1–D_7 for water, MEA, DEA, MDEA, and DGA are given in Table II. The vapor pressure has the unit of Pascals while temperature is expressed in Kelvins. Molar volumes for alkanolamines were estimated by the modified correlation of Rackett (*cf.* Ref. 18),

$$v_s = \frac{RT_c}{P_c} Z_{RA}^{[1-(1-T_r)^{2/7}]}, \qquad (17)$$

where Z_{RA} is a characteristic constant for each compound. Molar volume of water was taken from steam table data [19]. Relevant pure-component properties for molecular species are presented in Table III.

2.3. Reference states

In this work, both water and alkanolamines are treated as solvents. Consequently, the standard state associated with each solvent is the liquid pure at the system temperature and pressure. For ionic solutes, the adopted standard state is the ideal, infinitely dilute aqueous solution (infinitely dilute in solutes and alkanolamine) at the system temperature and pressure. The reference state chosen for molecular solutes (H_2S and CO_2) is also the ideal, infinitely dilute aqueous solution at the system temperature and pressure. This leads to the following unsymmetric convention for normalization of activity coefficients: for solvents, $\gamma_s \to 1$ as $x_s \to 1$; for ionic and molecular (neutral) solutes, $\gamma_i^* \to 1$ as $x_w \to 1$, where the subscript s refers to any nonaqueous solvent, i refers to ionic or neutral solutes, and w refers to water. Activity coefficients of all species are assumed to be independent of pressure.

2.4. Fugacity coefficients

In this work, the vapor-phase fugacity coefficients for molecular solutes, $\hat{\phi}_i$, and solvent species, $\hat{\phi}_s$ and $\hat{\phi}_s^\circ$, in Eqs. (11)

and (15) were calculated by using the Peng-Robinson cubic equation of state [20],

$$P = \frac{RT}{v-b} - \frac{a}{v(v+b)+b(v-b)} \tag{18}$$

although any other equation could be used as well. In this equation, P, T, v, and R are the pressure, temperature, molar volume, and a gas constant, respectively.

For pure components, parameters a and b are expressed in the usual way as a function of critical properties and acentric factors,

$$a = 0.457235\frac{R^2T_c^2}{P_c}\alpha(T), \tag{19}$$

$$b = 0.077796\frac{RT_c}{P_c}. \tag{20}$$

Since it is important that the pure component vapor pressures be correct for accurate vapor-liquid calculations and since some of the components considered here do not fit the generalized correlation for the equation of state parameters of Peng-Robinson equation, we use instead the correlation of Stryjek and Vera [21] to calculate parameter $\alpha(T)$,

$$\alpha(T) = \left\{1 + \kappa\left[1 - \left(\frac{T}{T_c}\right)^{0.5}\right]\right\}^2, \tag{21}$$

$$\kappa = \kappa_o + \kappa_1\left[1 + \left(\frac{T}{T_c}\right)^{0.5}\right]\left(0.7 - \frac{T}{T_c}\right), \tag{22}$$

with

$$\kappa_o = 0.378893 + 1.4897153\,\omega - 0.17131848\,\omega^2 + 0.019655\,\omega^3, \tag{23}$$

where κ_1 is a constant specific for each fluid, and they are also given in Table III. We refer to this as the PRSV equation of state.

For mixtures, parameters a and b are given by

$$a = \sum_i \sum_j x_i x_j \sqrt{a_i a_j}(1 - k_{ij}), \tag{24}$$

$$b = \sum_i x_i b_i, \tag{25}$$

where k_{ij} is the interaction parameter characterizing the binary i and j. For the H_2S-CO_2-water-alkanolamine system, these interaction parameters were fixed at zero, except for the binary H_2S-CO_2 where this parameter was set equal to 0.1.

For the PRSV equation of state and the mixing rules given by Eqs. (24) and (25), the fugacity coefficient of component i in a mixture can be written as

$$\ln\hat{\phi}_i = \frac{b_i}{b}(z-1) - \ln(z-B) - \frac{A}{2\sqrt{2}B}\left(\frac{2\sum_j x_j a_{ij}}{a} - \frac{b_i}{b}\right)\ln\frac{z+(1+\sqrt{2})B}{z+(1-\sqrt{2}B}, \tag{26}$$

where z is the compressibility factor defined as,

$$z = \frac{Pv}{RT} \tag{27}$$

and

$$A = \frac{aP}{R^2T^2}, \quad B = \frac{bP}{RT}. \tag{28}$$

2.5. Activity coefficients

The Electrolyte-NRTL model of Chen and Evans [12], modified for mixed solvent electrolyte solutions (see Ref. 14), was used to represent liquid phase activity coefficients. This is a generalized model of the excess Gibbs energy, which allows accounting for both ionic and molecular interactions between all true liquid-phase species. In general, the modified Electrolyte-NRTL model assumes that the excess Gibbs energy of a mixed solvent electrolyte solutions can be expressed as the sum of two contributions, one related to the local or short-range (ion-molecule, ion-ion, molecule-molecule) interactions that exist in the immediate neighborhood of any component (ion or neutral molecule), and the other related to the long-range ion-ion interactions that exist beyond the immediate neighborhood of a central ionic species, *i.e.*,

$$\frac{g^{ex^*}}{RT} = \frac{g^{ex^*}_{LR}}{RT} + \frac{g^{ex^*}_{local}}{RT}, \tag{29}$$

For the long-range ion-ion interactions, Chen and Evans [12] adopted the modified Pitzer-Debye-Hückel equation [22],

$$\frac{g^{ex^*}_{PDH}}{RT} = -\left(\sum_k x_k\right)\left(\frac{1000}{M_m}\right)^{\frac{1}{2}} \times \left(\frac{4A_\phi I_x}{\rho}\right)\ln(1+\rho I_x^{\frac{1}{2}}), \tag{30}$$

where M_m is the average molecular weight of water plus nonaqueous solvents, I_x is the ionic strength on mole fraction scale,

$$I_x = \frac{1}{2}\sum_i z_i^2 x_i, \tag{31}$$

and A_ϕ is a function of the mixed solvent dielectric constant, D_m, and mixed solvent density, d_m, which is estimated by

$$A_\phi = \frac{1}{3}\left(\frac{2\pi N_o d_m}{1000}\right)^{\frac{1}{2}}\left(\frac{e^2}{D_m kT}\right)^{\frac{3}{2}}, \tag{32}$$

with

$$d_m = (x^{sf}_{H_2O} v_{H_2O} + x^{sf}_{nonaq} v_{nonaq})^{-1}, \tag{33}$$

where v_{H_2O} is the molar volume of saturated water and v_{nonaq} is the saturation molar volume of the nonaqueous solvent fraction (*i.e.*, alkanolamine or mixture of amines), while $x^{sf}_{H_2O}$ and x^{sf}_{nonaq} are the solute-free mole fractions of water and total nonaqueous solvent, respectively.

TABLE IV. Temperature dependence of dielectric constants of alkanolamines.

Alkanolamine	A	B
Dielectric constants: $D = A + B(1/T - 1/373.15)$		
MEA[a]	36.76	14836.0
DEA[a]	28.01	9277.0
MDEA[b]	24.74	8989.3
DGA[c]	28.01	9277.0

[a] Austgen *et al.* [14] [b] Austgen [34]
[c] Coefficients fixed at same value as DEA

In order to make the Pitzer-Debye-Hückel contribution, Eq. (31), consistent with the adopted reference state for ions (the infinitely dilute aqueous solution), the Born equation (see Ref. 23) was introduced into the long-range contribution to account for the excess Gibbs energy of transferring an ion at infinite dilution in the mixed solvent to infinite dilution in the aqueous phase,

$$\frac{g^{\text{ex}}_{\text{Born}}}{RT} = \frac{e^2}{2kT}\left(\frac{1}{D_m} - \frac{1}{D_w}\right)\left(\sum_i \frac{x_i z_i^2}{r_i}\right) \times 10^{-2}, \quad (34)$$

where e is the electronic charge (4.803×10^{-10} esu), z_i is the valence of ionic species i, r_i is the radius of ionic species i, D_w is the dielectric constant of pure water estimated by the correlation of Helgeson and Kirkham [24], and D_m represents the dielectric constant of the mixed solvents which can be estimated by the following linear mass fraction average mixing rule,

$$D_m = \sum_i x_i^{\text{sf}} D_i, \quad (35)$$

where x_i^{sf} is the solute-free mass fraction of solvent i, and D_i is the dielectric constant of solvent i. Table IV presents the dielectric constants for all alkanolamines as a function of temperature. It should be noted that Eq. (34) was derived from consideration of the work required to transferring an ion from a solvent of dielectric constant D_m to dielectric constant D_w at extreme dilution.

Expressions for the excess Gibbs energy are generally developed with respect to symmetrically normalized activity coefficients; however, if the ideal dilute state is to be used as the reference state for solutes leading to unsymmetrically normalized activity coefficients, then the excess Gibbs energy must also be normalized to reflect the standard state of both solvent and solutes. Following Prausnitz and Chueh [25], the unsymmetric excess Gibbs energy is defined by

$$\frac{g^{\text{ex}^*}}{RT} = \sum_{\substack{\text{all solvent}\\ \text{components}}} x_i \ln \gamma_i + \sum_{\substack{\text{all solute}\\ \text{components}}} x_i \ln \gamma_i^*. \quad (36)$$

If the unsymmetrically normalized activity coefficients are expressed in terms of the respective symmetrically normalized activity coefficients, then Eq. (36) can be written as

$$\begin{aligned}\frac{g^{\text{ex}^*}}{RT} &= \sum_{\substack{\text{all solvent}\\ \text{components}}} x_i \ln \gamma_i + \sum_{\substack{\text{all solute}\\ \text{components}}} x_i (\ln \gamma_i - \ln \gamma_i^\infty) \\ &= \sum_{\text{all components}} x_i \ln \gamma_i - \sum_{\substack{\text{all solute}\\ \text{components}}} x_i \ln \gamma_i^\infty \quad (37)\end{aligned}$$

where γ_i^∞ is the symmetrically normalized activity coefficient of solute i at infinite dilution in the solvent, *i.e.*, $\gamma_i^\infty = \lim_{x_i \to 0} \gamma_i$. Thus, the unsymmetrically normalized excess Gibbs energy can be related to its symmetrically normalized counterpart by

$$\frac{g^{\text{ex}^*}}{RT} = \frac{g^{\text{ex}}}{RT} - \sum_{\substack{\text{all solute}\\ \text{components}}} x_i \ln \gamma_i^\infty \quad (38)$$

Using this equation, the long-range contribution to the excess Gibbs energy can then be expressed as

$$\frac{g^{\text{ex}^*}_{\text{LR}}}{RT} = \frac{g^{\text{ex}^*}_{PDH}}{RT} - \sum_i x_i \ln \gamma^\infty_{i,\text{Born}}, \quad (39)$$

where the symmetrically normalized activity coefficient of solute i at infinite dilution in the solvent, $\gamma^\infty_{i,\text{Born}}$, is given in Appendix A.

The local contribution to the excess Gibbs energy derived by Chen and Evans [12] was based on the local composition concept of the nonrandom two-liquid hypothesis proposed by Renon and Prausnitz [26]. In a straightforward extension of the original NRTL theory, these authors adopted an electrolyte solution to be consisted of three types of cells: one type consisting of a central neutral molecule surrounded by other molecules as well as anions and cations, where it is assumed that the distribution of cations and anions around a central solvent molecule is such that the net local ionic charge is zero (local electroneutrality assumption), while the other two types of cells have either a cation or an anion at the center which are surrounded by molecules and oppositely charged ions, but not by ions of the same charge type (like-ion repulsion assumption). This implies that the local concentration of cations (anions) around cations (anions) is zero. Therefore, the NRTL contribution to the excess Gibbs energy is expressed as

$$\begin{aligned}\frac{g^{\text{ex}}_{\text{NRTL}}}{RT} &= \sum_m X_m \frac{\sum_j X_j G_{jm} \tau_{jm}}{\sum_k X_k G_{km}} \\ &+ \sum_c X_c \sum_{a'} \frac{X_{a'} \sum_j G_{jc,a'c} \tau_{jc,a'c}}{\sum_{a''} X_{a''} \sum_k X_k G_{kc,a'c}} \\ &+ \sum_a X_a \sum_{c'} \frac{X_{c'} \sum_j G_{ja,c'a} \tau_{ja,c'a}}{\sum_{c''} X_{c''} \sum_k X_k G_{ka,c'a}} \quad (40)\end{aligned}$$

with

$$G_{cm} = \frac{\sum_a X_a G_{ca,m}}{\sum_{a'} X_{a'}}, \quad G_{am} = \frac{\sum_c X_c G_{ca,m}}{\sum_{c'} X_{c'}}, \tag{41}$$

$$\alpha_{cm} = \frac{\sum_a X_a \alpha_{ca,m}}{\sum_{a'} X_{a'}}, \quad \alpha_{am} = \frac{\sum_c X_c G_{ca,m}}{\sum_{c'} X_{c'}}, \tag{42}$$

and

$$G_{jc,a'c} = \exp(-\alpha_{jc,a'c}\tau_{jc,a'c}),$$
$$G_{ja,c'a} = \exp(-\alpha_{ja,c'a}\tau_{ja,c'a}), \tag{43}$$
$$G_{ca,m} = \exp(-\alpha_{ca,m}\tau_{ca,m}),$$
$$G_{im} = \exp(-\alpha_{im}\tau_{im}), \tag{44}$$
$$\alpha_{ma,ca} = \tau_{am} - \tau_{ca,m} + \tau_{m,ca},$$
$$\alpha_{mc,ac} = \tau_{cm} - \tau_{ca,m} + \tau_{m,ca}, \tag{45}$$

where $X_j = x_j C_j$ ($C_j = Z_j$ for ions and $C_j = 1$ for molecules), α is the nonrandomness parameter, and τ is the binary energy interaction parameter.

Since Eq. (40) reduces to the original NRTL model [26] when no ionic species are present in the solution, then binary interaction parameters for nonionic pairs can be obtained from analysis of the corresponding nonelectrolyte mixtures.

It should be pointed out that the NRTL contribution to the excess Gibbs energy, $g^{\text{ex}}_{\text{NRTL}}$, must also be normalized to the desired reference states using Eq. (38) and infinite dilution activity coefficients of molecular solutes, cations, and anions Therefore, the NRTL contribution to the unsymmetric excess Gibbs energy becomes

$$\frac{g^{\text{ex}^*}_{\text{NRTL}}}{RT} = \frac{g^{\text{ex}}_{\text{NRTL}}}{RT} - \sum_{m \neq w} x_m \ln \gamma^{\infty}_m - \sum_c x_c \ln \gamma^{\infty}_c - \sum_a x_a \ln \gamma^{\infty}_a, \tag{46}$$

where γ^{∞}_m, γ^{∞}_c, and γ^{∞}_a are the symmetrically normalized activity coefficients of, respectively, molecular solutes, cations, and anions at infinite dilution in the solvent. The subscript w refers to water. Thus, the sum of Eqs. (39) and (46) constitute the Electrolyte-NRTL equation for mixed solvent electrolyte system,

$$\frac{g^{\text{ex}^*}}{RT} = \left(\frac{g^{\text{ex}^*}_{\text{PDH}}}{RT} - \sum_i x_i \ln \gamma^{\infty}_{i,\text{Born}} \right) + \frac{g^{\text{ex}^*}_{\text{NRTL}}}{RT}. \tag{47}$$

Activity coefficient for ionic, molecular, solute, and solvent species, can be obtained by applying the following thermodynamic equation:

$$\ln \gamma_i = \left[\frac{\partial (n_t g^{\text{ex}} / RT)}{\partial n_i} \right]_{P,T,n_{j \neq i}} \tag{48}$$

All activity coefficients derived by the use of this equation are presented in Appendix A.

3. Solution approach

In this section, the developed algorithm to represent vapor-liquid equilibria data for the acid gas-alkanolamine-water system is described. The algorithm, similar to that of Austgen *et al.* [14], can be used to calculate total pressure and vapor partial pressure of all molecular components, given the temperature, T, the vector of liquid phase apparent mole fractions of water and all alkanolamines on an acid gas free basis, $\mathbf{x}^{\text{agf}}_a$, and the vector of loading, $\boldsymbol{\alpha}$, of H_2S and/or CO_2, in moles of acid gas per mole total alkanolamine (this quantity must be not confused with the nonrandomness parameter of the NRTL equation). It is worth noting that the mole fraction of any component is its mole fraction calculated by assuming that no reaction occurs in the liquid phase (apparent mole fraction of all ions are zero). $\mathbf{x}^{\text{agf}}_a$ is the vector of solvent mole fractions corresponding to the alkanolamine concentration of interest.

The algorithm is divided into two subalgorithms: the chemical equilibrium algorithm, which is responsible for determining the true composition of the liquid phase at equilibrium given temperature and the apparent composition of the liquid phase (*i.e.*, composition of the liquid phase corresponding to the equilibrium distribution of species), and the phase equilibrium algorithm, which is used to calculate the total pressure, P, and the vapor composition, y, once the equilibrium distribution of components in the liquid phase has been determined.

3.1. Chemical equilibrium algorithm

In general, to solve for the equilibrium composition of a system composed of N species and for which R independent reactions can be written, nonlinear algebraic equations of the form as given by Eqs. (9) and $N - R$ linear algebraic equations representing mass balances, must be simultaneously solved for N equilibrium values of x_i. This traditional approach is sometimes classified as a stoichiometric formulation of the equilibrium problem in which the closed-system constraints and the elemental balance equations are treated by means of stoichiometric equations leading to an unconstrained minimization of the Gibbs free energy problem. However, this problem can be reformulated in such a way that fewer equations must be solved simultaneously so that Eqs. (9) are not used directly to solve for the liquid phase equilibrium composition. Toward this end, the approach adopted in this work was that developed by Smith and Missen [27]. This approach, classified as a nonstoichiometric formulation of the equilibrium problem, is based on constrained minimization of the Gibbs free energy, *i.e.*, at a constant temperature and pressure, the most stable state of a system is the state at which the Gibbs free energy, G, is a minimum.

Therefore, the condition of chemical equilibria can be found by minimizing G, at constant temperature and pressure, in terms of $\mathbf{n}$ mole numbers and subject to M elemental balance constraints,

$$\min G(\mathbf{n}) = \sum_{i=1}^{N} n_i \mu_i, \tag{49}$$

subject to

$$\sum_{i=1}^{N} a_{ki} n_i = b_k, \qquad k = 1, \ldots, M, \tag{50}$$

where N is the number of components in the system (excluding inerts), M is the number of elements in the system, a_{ki} is the subscript to the k-th element in the molecular formula of species i, and b_k is some fixed amount of element k in the system.

In the Smith and Missen algorithm, the constrained minimization problem is transformed into an unconstrained minimization problem by formulating the Lagrangian from Eqs. (49) and (50), *i.e.*,

$$L(\mathbf{n}, \boldsymbol{\lambda}) = \sum_{i=1}^{N} n_i \mu_i + \sum_{i=1}^{M} \lambda_k (b_k - \sum_{i=1}^{N} a_{ki} n_i), \tag{51}$$

where $\boldsymbol{\lambda}$ is a vector of M unknown Lagrange multipliers, $\boldsymbol{\lambda} = (\lambda_1, \ldots, \lambda_M)^T$. By applying the necessary conditions for a minimum in $L(\mathbf{n}, \boldsymbol{\lambda})$, we have

$$\mu_i - \sum_{k=1}^{M} a_{ki} \lambda_k = 0, \qquad i = 1, \ldots, N, \tag{52}$$

$$b_k - \sum_{i=1}^{N} a_{ki} n_i = 0, \qquad k = 1, \ldots, M. \tag{53}$$

Equations (52) and (53) represent a set of $N + M$ nonlinear algebraic equations in $N + M$ unknowns $(n_1, \ldots, n_N, \lambda_1, \ldots, \lambda_M)$. However, these equations are difficult to solve due to the nonlinear dependence of the chemical potentials on mole number. To overcome this problem, Smith and Missen adopted an iterative procedure whereby Eqs. (52) are linearized in mole numbers by expansion in a Taylor series truncated after the linear term, and used with Eqs. (53) to solve for mole numbers. The procedure is then repeated until the difference between mole numbers of the constituents on consecutive iterations is less than a prescribed convergence criterion. Briefly, linearization of Eqs. (52) about an estimate of the equilibrium state solution $(\mathbf{n}^{(m)}, \Psi^{(m)})$ gives,

$$\frac{\mu_i^{(m)}}{RT} - \sum_{k=1}^{M} a_{ki} \Psi^{(m)} + \frac{1}{RT} \sum_{j=1}^{N} \left(\frac{\partial \mu_i^{(m)}}{\partial n_j} \right) \delta n_j^{(m)} - \sum_{k=1}^{M} a_{ki} \delta \Psi_k^{(m)} = 0, \qquad i = 1, \ldots, N, \tag{54}$$

with

$$\delta n_j^{(m)} = n_j - n_j^{(m)} \tag{55}$$

and

$$\delta \Psi_k^{(m)} = \Psi_k - \Psi_k^{(m)}, \tag{56}$$

where the subscript (m) denotes evaluation at the point $(\mathbf{n}^{(m)}, \Psi^{(m)})$ and $\Psi = \lambda_k / RT$. $\mathbf{n}$ is related to the current estimate of $\mathbf{n}^{(m)}$ through the elemental abundance constraints, [Eqs. (50)], by

$$\sum_{j=1}^{N} a_{kj} \delta n_j^{(m)} = b_k - b_k^{(m)}, \qquad k = 1, \ldots, M, \tag{57}$$

where

$$b_k^{(m)} = \sum_{j=1}^{N} a_{kj} n_j^{(m)}, \qquad k = 1, \ldots, M. \tag{58}$$

Equations (54) and (55) are a set of $N + M$ linear equations in the unknowns $\delta n_j^{(m)}$ and $\delta \Psi_k^{(m)}$, which can be reduced to a system of M linear equations in M unknowns by combining Eqs. (54) and (57) to yield an explicit expression for the variables $\delta \mathbf{n}^{(m)}$. That is, introducing the expression of the chemical potential of an ideal solution, defined as

$$\mu_i = \mu_i^{\circ}(T, P) + RT \ln x_i, \quad (x_i = n_i / n_t) \tag{59}$$

into Eq. (54), and rearranging yields

$$\delta n_j^{(m)} = n_j^{(m)} \left(-\frac{\mu_i^m}{RT} + \Gamma + \sum_{k=1}^{M} a_{ki} \Psi_k^{(m)} \right), \qquad j = 1, \ldots, N, \tag{60}$$

with

$$\Gamma = \sum_{j=1}^{N} \frac{\delta n_j^{(m)}}{n_t^{(m)}} = \frac{\delta n_t^{(m)}}{n_t^{(m)}}, \tag{61}$$

where n_t represents total moles in the phase including inerts. Introducing Eq. (60) into the modified element abundance constraint, [Eq. (57)], and after rearrangement, we have

$$\sum_{i=1}^{M} \sum_{j=1}^{N} \left(a_{kj} a_{ij} n_j^{(m)} \right) \Psi_i + b_k^{(m)} \Gamma = \left[\frac{1}{RT} \sum_{j=1}^{N} a_{kj} n_j^{(m)} + (b_k - b_k^{(m)}) \right], \qquad k = 1, \ldots, M. \tag{62}$$

Summing Eqs. (60) over j (the number of components excluding inerts) and using Eq. (61), yields

$$\sum_{i=1}^{M} b_i^{(m)} \Psi_i - n_{\text{inerts}} \Gamma = \frac{1}{RT} \sum_{k=1}^{N} n_k^{(m)} \mu_k^{(m)}, \qquad (63)$$

where n_{inerts} is the number of inert components.

Equations (62) and (63) represent a system of $M+1$ equations in $M+1$ unknowns, the M Lagrange multipliers, Ψ_i, and Γ. Nonetheless, as suggested by Smith and Missen, a system of M equations in M unknowns can be obtained by setting Γ to zero. These authors proved that this variation still leads to a descent algorithm.

It should be noted that the nonstoichiometric algorithm presented above was developed for ideal solutions, [Eq. (59)], in which it is possible to express $\partial \mu_i / \partial n_j$ analytically. Therefore, in order to use algorithms for nonideal solutions, Smith and Missen used an indirect approach. That is, the chemical potential for a nonideal solution is expressed as

$$\mu_i = \mu_i^{\circ}(T, P) + RT \ln \gamma_i(T, P, \mathbf{n}) + RT \ln x_i. \qquad (64)$$

Combining the first two terms, Eq. (64) can formally be written as,

$$\mu_i = \mu_i^{\circ}(T, P, \mathbf{n}) + RT \ln x_i \qquad (65)$$

where μ_i° is now a function of T and P through the unknown equilibrium solution $\mathbf{n}$. The calculation procedure is iterative. On the first iteration, the equilibrium composition is calculated assuming an ideal behavior, *i.e.*, $\gamma_i = 1$ and $\mu_i^{\circ}(T, P, \mathbf{n}) = \mu_i^{\circ}(T, P)$, obtaining the mole numbers of the system, $\mathbf{n}^{(1)}$. Using the composition of the system on the first iteration, activity coefficients are calculated for all species through the excess Gibbs energy function. On the next iteration, a new value of $\mu_i^{\circ}(T, P, \mathbf{n})$ is computed by Eq. (65) such that

$$\mu_i^{\circ(1)} = \mu_i^{\circ} + RT \ln \gamma_i(T, P, \mathbf{n}^{(1)}). \qquad (66)$$

Note that in applying the approach for an ideal solution, $\mu_i^{\circ(m)}$ is not treated as function of composition, *i.e.*, $\partial \mu_i^{\circ(m)} / \partial n_j$ is assumed to be zero. The procedure is repeated until the composition does not change significantly on consecutive iterations, so that Eq. (66) becomes

$$\mu_i^{\circ(m)} = \mu_i^{\circ} + RT \ln \gamma_i(T, P, \mathbf{n}^{(m)}), \quad m = 1, 2, \ldots. \qquad (67)$$

The algorithm described above for calculating the equilibrium composition of the system requires from the knowledge of the standard state chemical potentials, μ_i°, for all species participating in the independent set of chemical reactions. Equations (9) provides a connection between standard state chemical potentials for all components participating in a reaction and the equilibrium constant for that reaction,

$$RT \ln K_j = -\sum_{i=1}^{N} \nu_{ij} \mu_i^{\circ} \quad j = 1, \ldots, R \qquad (68)$$

Here, the main problem is to determine a suitable vector $\boldsymbol{\mu}^{\circ}$ which gives the correct value of $\mathbf{K}$ through Eqs. (68) to obtain the correct equilibrium composition of the system. Therefore, for a system consisting of N species and R independent reactions, any vector $\boldsymbol{\mu}^{\circ}$ which satisfies Eqs. (68) can be used to determine the equilibrium composition of the system by the nonstoichiometric algorithm. Since N is generally greater than R, then there are an infinite number of vectors μ° that are consistent with the j values of $\mathbf{K}$. One such a vector results from setting $N - R$ values of $\boldsymbol{\mu}^{\circ}$ to zero and using Eqs. (68) to solve for the remaining R values. This single method was used here to determine a consistent set of $\boldsymbol{\mu}_i^{\circ} (i = 1, \ldots, N)$.

The chemical equilibrium algorithm used in this work for determining the true mole liquid phase composition can be summarized as follows: given the temperature, T, apparent mole fractions of all solvents on an acid gas free basis, $\mathbf{x}_a^{\text{agf}}$, the acid gas loading α_{H_2S} and/or α_{CO_2}, the element abundance matrix, $\mathbf{A}$, and the stoichiometric coefficient matrix, $\mathbf{N}$, for a set of independent chemical reactions, R, all thermodynamic variables that depend on temperature, $\mathbf{K}(T)$, $P^{\circ}_{\text{solvent}}(T)$, $H^{\circ}_{\text{acid gas}}(T)$, are determined on the first iteration of each bubble point calculation. From the equilibrium constants, a suitable set of standard-state chemical potentials is calculated from the procedure outlined above. Apparent mole fractions of the acid gases are then determined from the acid gas free apparent mole fractions of alkanolamines and the acid gas loading (in moles of acid gas per mole of total amine).

Assuming a total of one mole of the liquid phase on an apparent basis, the apparent mole fractions are mapped into the true mole number vector. All other mole numbers (*i.e.*, mole numbers of all ionic species) are set to an arbitrary small number, which serves as an initial estimate of the true mole numbers. Apparent mole numbers of water, all alkanolamines, and all acid gases are used to calculate the total mole numbers of all elements by Eqs. (50). Here, the elements are taken to be H, O, C, S, and amine rather than N, to simplify the element abundance matrix, $\mathbf{A}$.

From the initial guess of the true mole number vector, the chemical potentials of all species are calculated by Eq. (59). Thus, given the initial estimates of all mole numbers and all chemical potentials as well as the element abundance and stoichiometric coefficient matrices, $\mathbf{A}$ and $\mathbf{N}$, the Smith and Missen algorithm was applied to update the mole numbers which, in turn, are used to calculate the chemical potentials. The mole fractions of all liquid phase species are renormalized on each iteration so that $\sum_{i=1}^{N} x_i = 1$. Iterations are continued until true mole numbers do not change significantly on consecutive iterations. That is, convergence is achieved when

$$\max \left| \frac{\delta n_i^{(m)}}{n_i^{(m)}} \right| \leq 10^{-6}, \text{ for all } i, \qquad (69)$$

where n_i is the true mole number of component i and $\delta n_i^{(m)}$ is given by Eq. (60). The converged mole number vector in

conjunction with temperature are used to calculate a new estimate of the activity coefficients of all species by using the Electrolyte-NRTL equation. The new estimate of the activity coefficient vector is used to calculate a new true mole fraction vector. This calculation is repeated until the mole numbers of all species do not change significantly on consecutive iterations, *i.e.*, convergence is attained when,

$$\max \left| \frac{n_i^{(m+1)} - n_i^{(m)}}{n_i^{(m)}} \right| \leq 10^{-6}, \text{ for all } i. \qquad (70)$$

3.2. Phase equilibrium algorithm

Once having calculated the true liquid phase composition and activity coefficient vector, then the phase equilibrium algorithm is applied to calculate the vapor phase composition by using this information together with Eqs. (11) and (15). In this algorithm, the total pressure is needed for determination of the fugacity coefficients of all vapor phase species, $\phi_i(T, P, y)$, as well as for evaluation of the exponential terms in these expressions, *i.e.*, the Poynting pressure correction factors.

Initially, the vapor phase fugacity coefficients and Poynting factors of all molecular components are set to unity while the total pressure is set to zero. The phase equilibrium algorithm is then applied to determinate an initial estimate of the partial pressures, p_i, of all molecular components by Eqs. (11) and (15). The total pressure, $P = \sum_i p_i$, and vapor mole fractions, $y_i = p_i/P$ (i $= 1, \ldots, N$) , which satisfy $\sum_{i=1}^{N} y_i = 1$, are then calculated. Using the estimate of P, the Poynting pressure correction term in Eqs. (11) and (15) are evaluated and the liquid standard state fugacities are adjusted for the effect of pressure. The partial pressures of all molecular species are then recalculated and a new estimate of the total pressure is made.This iterative calculation continue until convergence is achieved when

$$\left| \frac{P^{(m+1)} - P^{(m)}}{P^{(m)}} \right| \leq 10^{-4}. \qquad (71)$$

From the converged estimates of P and $y_i (i = 1, \ldots, N)$, the fugacity coefficients, $\phi_i(T, P, y)$, of all species are re-estimated using the PRSV equation of state. The updated fugacity coefficients are then used to give new estimates of total pressure and vapor phase composition. Again, iterations continue until attain the following convergence criterion

$$\max \left| \frac{y_i^{(m+1)} - y_i^{(m)}}{y_i^{(m)}} \right| \leq 10^{-6}, \text{ for all } i. \qquad (72)$$

4. Data regression

The parameters required by the Electrolyte-NRTL equation for the acid gas-alkanolamine-water system include the distance of closest approach, ρ, in the Pitzer-Debye-Hückel term, Eq. (31), and pure-component dielectric constants, D_i, and ionic radii, r_i, in the Born term, Eq. (34), while the parameters in the NRTL term, Eq. (40), are the binary parameters, τ_{ij}, and the nonrandomness factors, α_{ij}. In this work, the closest approach parameter was setting to 14.9 [14] while default values of 3Å were assigned to all the ionic radii.

For the NTRL equation, there are three types of binary interaction parameters that represent the energies of interaction between liquid phases species: molecule-molecule ($\tau_{m,m'}$ and $\tau_{m',m}$), molecule-ion pair ($\tau_{m,ca}$ and $\tau_{ca,m}$), ion pair-ion pair with a common cation ($\tau_{ca,ca'}$ and $\tau_{ca',ca}$), and ion pair-ion pair with a common anion ($\tau_{ca,c'a}$ and $\tau_{c'a,ca}$). In order to reduce the data regression problem for mixed-solvent electrolyte systems to the determination of molecule-molecule and molecule-ion pair parameters only, the ion pair-ion pair ($\tau_{ca,ca'}, \tau_{ca',ca}, \tau_{ca,c'a}, \tau_{c'a,ca}$) parameters were set to zero. Chen and Evans [12] showed that this assumption does not affect significantly the representation of the vapor-liquid equilibrium data. In addition, the nonrandomness parameters, α_{ij}, were fixed at 0.2 for molecule-molecule ($\alpha_{mm'}$) and water-ion pair ($\alpha_{w,ca}$ or $\alpha_{ca,w}$) interactions, while for alkanolamine-ion pair and acid gas-ion pair interactions, these parameters were setting to 0.1 (see Refs. 10 and 28). Hence, the only adjustable parameters of the Electrolyte-NRTL equation are the molecule-molecule ($\tau_{m,m'}$ and $\tau_{m',m}$), and molecule-ion pair ($\tau_{m,ca}$ and $\tau_{ca,m}$) interaction parameters.

Vapor-liquid equilibrium data were regressed to obtain a set of interaction parameters characterizing the interactions between species, which were assumed to be temperature dependent according to the following function:

$$\tau = a + b/T. \qquad (73)$$

The optimum values of constants a and b, including the estimation of the carbamate stability equilibrium constant, were obtained by minimization of the following objective function

$$S = \sum_{i=1}^{M} \left| \frac{P_i^{\text{exp}} - P_i^{\text{calc}}}{P_i^{\text{exp}}} \right|, \qquad (74)$$

where the term $P_i^{\text{exp}} - P_i^{\text{calc}}$ represents the residual between experimental and calculated bubble-point pressures for experiment i, and M is the total number of experimental measurements. The Simplex optimization method (see Ref. 29) was used for minimization of Eq. (74), subject to the vapor-liquid equilibrium constraints on acid gases, Eq. (11), and chemical equilibrium constraints for all reactions included in the model, Eq. (9).

The agreement between experimental and calculated pressures at the bubble-point of the mixture, was established through the absolute percent relative deviation in pressure, σ_p, given by

$$\sigma_p = \frac{100}{M} \sum_{i=1}^{M} \left| \frac{P_i^{\text{exp}} - P_i^{\text{calc}}}{P_i^{\text{exp}}} \right|, \qquad (75)$$

TABLE V. Electrolyte-NRTL parameters, $\tau = a + b/T$, for the alkanolamine-water and acid gas-water systems, and absolute percent relative deviation in pressure, σ_P.

Molecular pair	a	$b(K)$	σ_P
H_2O-MEA	1.0352	93.329	
MEA-H_2O	0.3237	−694.920	2.8
H_2O-MDEA	13.1980	−3554.40	
MDEA-H_2O	−2.7123	182.86	1.7
H_2O-DEA	−3.0740	1527.00	
DEA-H_2O[a]	0.5090	829.00	
H_2O-DGA	0.5840	418.00	
DGA-H_2O[a]	0.6130	−930.00	
H_2O-CO_2	10.0640	−3268.10	
CO_2-H_2O[b]	10.0640	−3268.10	
H_2O-H_2S	−3.6740	1155.90	
H_2S-H_2O[b]	−3.6740	1155.90	

[a] Chang *et al.* [30] [b] Chen y Evans [12]

where σ_p was obtained for each system by using the optimal values of the estimated interaction parameters.

4.1. Binary systems

For the acid gas-alkanolamine-water system, there exist three constituent binary subsystems, which can be formed: alkanolamine-water, acid gas-water, and acid gas-alkanolamine mixtures. Since the systems alkanolamine-water and acid gas-water are aqueous single weak electrolyte ones, and the degree of dissociation of electrolyte in each is negligible, except a high dilutions, then chemical equilibria can be ignored. Notwithstanding, to test the ability of our model in representing phase equilibria for such systems, we have correlated the vapor-liquid equilibrium data for MEA-H_2O and MDEA-H_2O systems. Results of the regression for these nonelectrolyte systems are presented in Table V. This table show that the data sets of these systems are fit well with absolute percent relative deviations in pressure, σ_P, of 2.8 and 1.7% for and MEA-H_2O and MDEA-H_2O, respectively. Austgen *et al.* [15] did not include fitted parameters for the binary MDEA-H_2O system. They set the parameters for MDEA-H_2O to the default value of zero. Table V also provides parameters for the binary molecular interactions. DEA-H_2O and DGA-H_2O parameters were taken from Chang *et al.* [30]. The acid gas-water parameters CO_2-H_2O and H_2S-H_2O) were taken from Chen and Evans [12] and all other unlisted binary interactions parameters were assumed to be zero. These parameter values were included in the full Electrolyte-NRTL model and were not re-regressed.

As outlined above, because the Electrolyte-NRTL equation reduces to the original NRTL model [26] when no ionic species are present in solution, then it is valid to assume that no ionic species are present in aqueous solutions of either an alkanolamine or an acid gas for purposes of modeling the vapor-liquid equilibria behavior of these binary systems. The NRTL binary interaction (molecule-molecule) parameters fitted on the binary system data are entirely consistent with corresponding parameters of the Electrolyte-NRTL equation. The NRTL equation also contains a single nonrandomness parameter corresponding to each pair of interaction parameters. Hence, to be consistent with the approach adopted for acid gas-alkanolamine-water system, these parameters were set to 0.2 for all binary molecular pairs.

4.2. Ternary systems

In order to determine the best values of the molecule-ion pair and ion pair-molecule parameters, the molecule-molecule interactions parameters were fixed at values estimated from binary (acid gas-water and alkanolamine-water) vapor-liquid equilibrium data. The thermodynamic model was then fitted to ternary (alkanolamine-acid gas-water) vapor-liquid equilibrium data. According to Austgen *et al.* [14], because there is a large body of H_2S and CO_2 solubility data reported for aqueous alkanolamine solutions, then only those solubility measurements published after 1956 were used in the estimation of molecule-ion pair parameters.

Since vapor-liquid equilibrium data for alkanolamine-acid gas-water systems are usually reported as equilibrium acid gas partial pressures and equilibrium acid gas loadings (*i.e.*, moles acid gas/mole amine) in an aqueous solution of specified amine concentration, then the molecule-ion pair parameters were fitted on acid gas phase equilibria only. Literature sources used in fitting all parameters are summarized in Table VI. An examination of the experimental data presented in this table shows that there is significant scatter of experimental data both within and between the different data sources. Thus, by using several sources of experimental data for parameter estimation, the best parameter values were determined to represent the data as a whole.

Fitted values of the coefficients of Eq. (73) for Electrolyte-NRTL binary molecule-ion pair and ion pair-molecule interaction parameters corresponding to the regression of the vapor-liquid equilibrium data for systems H_2S-MEA-H_2O, CO_2-MEA-H_2O, H_2S-DEA-H_2O, CO_2-DEA-H_2O, H_2S-DMEA-H_2O, CO_2-MDEA-H_2O, H_2S-DGA-H_2O, and CO_2-DGA-H_2O, are given in Table VII. This table also includes their corresponding absolute percent relative deviations in pressure, σ_P. Parameters not listed here were set to the default values given in Table VIII. That is, all water-ion pair and ion pair-water parameters were fixed at default values of 8.0 and −4.0, respectively, while all alkanolamine-ion pair and ion pair-alkanolamine, and all acid gas-ion pair and ion pair-acid gas binary parameters were fixed at default values of 15.0 and −8.0, respectively. The non-randomness parameter, α, was not regressed and was set to the default

TABLE VI. Sources of experimental vapor-liquid equilibrium data for estimating molecule-ion pair binary parameters in ternary acid gas-alkanolamine-water systems.

Reference	Amine concentration[a]	Temperature range(°C)	Acid gas loading range
	MEA-CO_2-H_2O		
Lee *et al.* [37]	1.0, 2.5, 3.75, 5.0 M	25–120	0.090–2.00
Isaac*et al.* [38]	2.5 M	80, 100	0.040–0.32
Lawson and Garst [39]	15.2, 30.0 wt%	40–140	0.110–1.00
Jones *et al.* [40]	15.3 wt%	40–140	0.130–0.73
Muhlbauer and Monaghan [41]	2.5 M	25, 100	0.460–0.74
	MEA-H_2S-H_2O		
Lee *et al.* [42]	2.5, 5.0 M	40, 100	0.120–1.55
Lee *et al.* [43]	2.5, 5.0 M	25–120	0.210–1.61
Lawson and Garst [39]	15.2, 30.0 wt%	40–140	0.005–1.63
Jones *et al.* [40]	15.3 wt%	40–140	0.025–0.97
Muhlbauer and Monaghan [41]	2.5 M	25, 100	0.200–0.93
	DEA-CO_2-H_2O		
Lee *et al.* [44]	0.5, 2.0, 3.5, 5.0 M	25–120	0.030–3.326
Lee *et al.* [45]	2.0 M	40, 100	0.005–0.37
Lawson and Garst [39]	25, 50 wt%	38–120	0.320–1.17
	DEA-H_2S-H_2O		
Lee *et al.* [46]	2.0, 3.5 M	25–120	0.070–1.55
Lee *et al.* [47]	0.5, 5.0 M	25–120	0.020–3.29
Lal *et al.* [45]	2.0 M	40–100	0.007–0.22
Atwood *et al.* [48]	10, 25, 50 wt%	27–60	0.005–1.00
Lawson and Garst [39]	25, 50 wt%	38–150	0.004–1.58
	MDEA-CO_2-H_2O		
Jou *et al.* [49]	2.0, 4.28 M	25–120	0.001–3.22
Jou *et al.* [50]	3.04 M	40, 100	0.002–0.80
Bhairi [51]	1.0, 2.0 M	25–116	0.160–1.51
	MDEA-H_2S-H_2O		
Jou *et al.* [49]	1.0, 2.0, 4.28 M	25–120	0.001–1.83
Jou *et al.* [50]	3.04 M	40, 80	0.004–1.08
Bhairi [51]	1.0, 2.0 M	25–116	0.180–2.17
	DGA-CO_2-H_2O		
Matin *et al.* [52]	60 wt%	50, 100	0.130–0.80
Dingman *et al.* [31]	65 wt%	38–82	0.003–0.59
	DGA-H_2S-H_2O		
Matin *et al.* [52]	60 wt%	50, 100	0.060–1.09
Dingman *et al.* [31]	65 wt%	38–82	0.003–0.85

[a] Amine concentrations are acid gas free

values recommended in Austgen *et al.* [14]. All default values were assumed to have no temperature dependence, *i.e.*, $b = 0$.

Figures 3 and 4 summarize the ratios of the calculated to the measured equilibrium partial pressures for CO_2-MEA-H_2O and H_2S-MEA- H_2O systems in the temperature range 25–120°C. Figures summarizing the ratios of the calculated to the experimental partial pressures for the other six ternary systems considered in this work show similar behavior so that they were not included here. In all, most of the vapor-liquid equilibrium data was fit within ±25%.

5. Model predictions

As stated earlier, the main goal of any developed model is to provide a means that can confidently be used for interpola-

TABLE VII. Electrolyte-NRTL parameters, $\tau = a + b/T$, for the H_2S-alkanolamine-H_2O and CO_2-alkanolamine-H_2O systems, and absolute percent relative deviation in pressure, σ_P.

System	No. data	a	$b(K)$	σ_P
H_2S-MEA-H_2O	184			13.5
H_2O-($MEAH^+$, HS^-)		6.9023	401.24	
($MEAH^+$, HS^-)-H_2O		−3.4406	−215.85	
CO_2S-MEA-H_2O	193			14.8
H_2O-($MEAH^+$, HCO_3^-)		4.0563	581.65	
($MEAH^+$, HCO_3^-)-H_2O		−2.8773	0.00	
H_2O-($MEAH^+$, $MEACOO^-$)		9.2732	0.00	
($MEAH^+$, $MEACOO^-$)-H_2O		−4.8766	0.00	
H_2S-DEA-H_2O	186			22.3
H_2O-($DEAH^+$, HS^-)		5.0738	1337.30	
($DEAH^+$, HS^-)-H_2O		−2.3518	−755.55	
CO_2-DEA-H_2O	174			18.5
H_2O-($DEAH^+$, HCO_3^-)		2.0153	1568.40	
($DEAH^+$, HCO_3^-)-H_2O		−2.4157	−423.80	
H_2O-($DEAH^+$, $DEACOO^-$)		7.9962	165.49	
($DEAH^+$, $DEACOO^-$)- H_2O		−3.8412	−186.20	
H_2S-MDEA-H_2O	182			24.0
H_2O-($MDEAH^+$, HS^-)		8.9443	−850.86	
($MDEAH^+$, HS^-)-H_2O		−5.7352	931.19	
CO_2-MDEA-H_2O	187			19.0
H_2O-($MDEAH^+$, HCO_3^-)		15.713	−2543.60	
($MDEAH^+$, HCO_3^-)-H_2O		−9.1233	1783.20	
H_2S-DGA-H_2O	100			22.5
H_2O-($DGAH^+$, HS^-)		7.0321	425.59	
($DGAH^+$, HS^-)-H_2O		−3.7153	−148.24	
CO_2-DGA-H_2O	80			16.1
H_2O-($DGAH^+$, HCO_3^-)		1.5759	1972.40	
($DGAH^+$, HCO_3^-)-H_2O		−2.8742	−290.50	
H_2O-($DGAH^+$, $DGACOO^-$)		9.7715	581.73	
($DGAH^+$, $DGACOO^-$)-H_2O		−4.5484	−291.56	

TABLE VIII. Default Electrolyte-NRTL parameters, $\tau = a + b/T$ ($b = 0$), specified in this work[a].

		a	α
H_2O	(ca)	8.0	0.2
(ca)	H_2O	−4.0	0.2
amine	(ca)	15.0	0.1
(ca)	amine	−8.0	0.1
solute	(ca)	15.0	0.1
(ca)	solute	−8.0	0.1
($c'a'$)	($c''a''$)	0.0	0.1
($c''a''$)	($c'a'$)	0.0	0.1
m_1	m_2	0.0	0.2
m_2	m_1	0.0	0.2

[a] Solute = CO_2 or H_2S, (ca) = cation, anion pair, m_1 = solvent or solute

tions of the data or extrapolations in regions beyond where measurements have been made. This is important due to the lack of experimental data at low acid gas partial pressure range where it is *a priori* most important for design gas treating operations.

Figures 5 and 6 show the model application to the prediction of CO_2 and H_2S equilibrium partial pressures as a function of acid gas loading of the liquid phase, respectively. These figures were generated at 50°C over 2.0 kmol m^{-3} MEA, DEA, MDEA, and DGA aqueous solutions using our model for the eight ternary systems considered above.

An inspection of Fig. 5 shows that at these conditions of temperature and total amine concentration, the CO_2 equilibrium partial pressure varies depending upon the acid gas loading. In particular, in the CO_2 loading range from 0.01 to 0.40, it is seen that the CO_2-MEA-H_2O system presents the lowest CO_2 equilibrium partial pressure while the CO_2-MDEA-

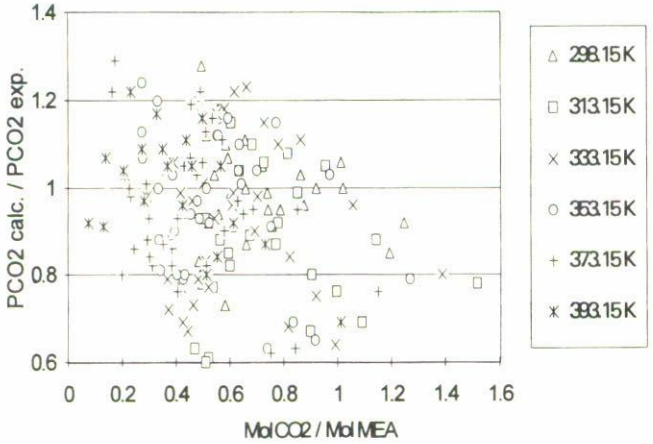

FIGURE 3. Regressed fit of CO_2 partial pressure data as a function of CO_2 loading for the CO_2-MEA-H_2O system.

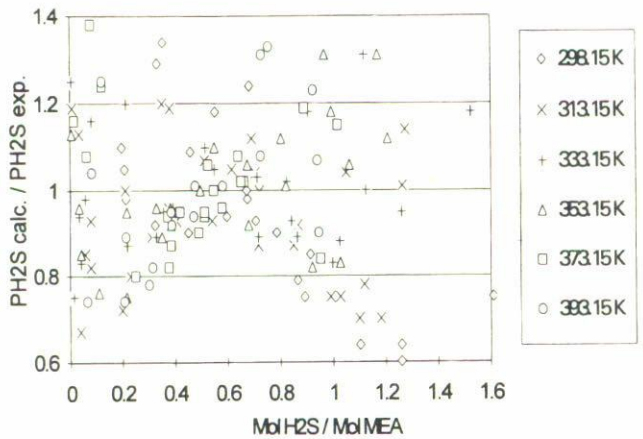

FIGURE 4. Regressed fit of H_2S partial pressure data as a function of H_2S loading for the H_2S-MEA-H_2O system.

H_2O system presents the highest one. This means that MEA and MDEA aqueous solutions have, respectively, a greater and a lower absorption capacity with respect to the other aqueous alkanolamine. On the contrary, in the CO_2 loading range from 0.40 to 0.75, the aqueous solution with DGA presents the lowest CO_2 equilibrium partial pressure.

Due to that MDEA does not react directly with CO_2 to form a carbamate, then we can expect that its capacity to absorb this acid gas is lower than for other three amines considered here. However, when the CO_2 loading is greater than 0.75 moles CO_2/mole of amine, then MDEA aqueous solution has a lower CO_2 equilibrium partial pressure than for other aqueous alkanolamines. For instance, if a sour gas containing a CO_2 loading of about 0.40 moles CO_2/mole of amine is introduced at the bottom of the absorber in an absorption/stripping operation at 50°C, the amines with lower CO_2 equilibrium partial pressure will be DGA and MDEA.

It should be noted that the complicated behavior shown for the CO_2-alkanolamine-H_2O systems is due to the formation of carbamate for MEA, DGA, and DEA, besides to the dissociation of CO_2. It is also known that the formation of carbamate dominates the chemical equilibria below loadings

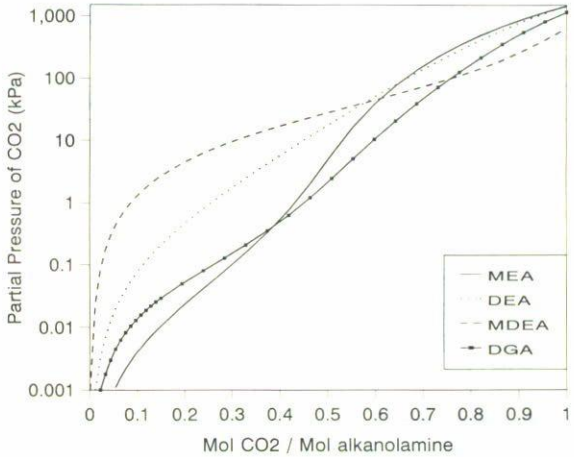

FIGURE 5. Model prediction of CO_2 equilibrium partial pressures at 50°C over 2.0 kmol m^{-3} MEA, DEA, MDEA, and DGA aqueous solutions as functions of acid gas loading in the liquid phase.

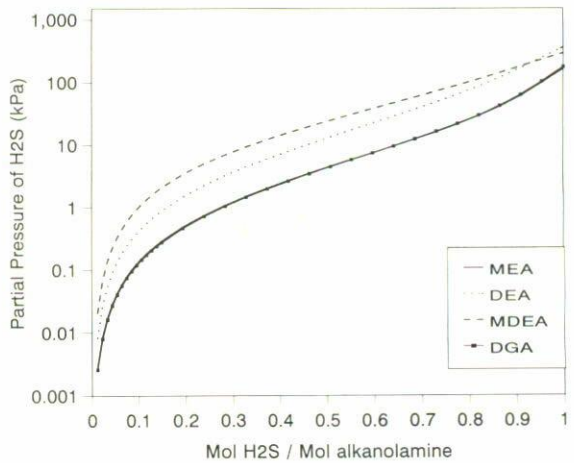

FIGURE 6. Model prediction of H_2S equilibrium partial pressures at 50°C over 2.0 kmol m^{-3} MEA, DEA, MDEA, and DGA aqueous solutions as functions of acid gas loading in the liquid phase.

of 0.5 moles CO_2/mole amine, and that reversion of carbamate to bicarbonate dominates equilibria above a loading of 0.5, as shown in Fig. 3.

Conversely, Fig. 6 clearly illustrates that the behavior for the H_2S-alkanolamine-H_2O systems is less complicated than that reported for the CO_2-alkanolamine-H_2O systems. This figure shows a regular trend of the H_2S equilibrium partial pressure for all alkanolamines considered here. This is because the H_2S does not react directly with the amine. This figure shows that in the H_2S loading range from 0 to 1 moles H_2S/mole amine, the H_2S equilibrium partial pressure curves are similar for the systems H_2S-MEA-H_2O and H_2S-DGA-H_2O, *i.e.*, the H_2S predicted equilibrium partial pressure curves for MEA and DGA are superimposed to each other.

Overall, it is seen that MEA and DGA aqueous solutions have the greatest absorption capacity, while the aqueous solution has the lowest one, along all the H_2S loading range.

6. Conclusions

A thermodynamic model was developed to represent vapor-liquid equilibrium data of acid gas (H_2S, CO_2)-alkanolamine(MEA, DEA, DGA, MDEA)-water systems. This model accounts for chemical equilibria in a rigorous fashion to determine the true compositions of all liquid-phase species, ionic and molecular, and phase equilibria to determine the equilibrium distribution of molecular species between the vapor and liquid phases. In general, the system is modeled as a solution of molecular and ionic solutes in a mixture of water and alkanolamines.

Liquid-phase activity coefficients were represented with the Electrolyte-NRTL equation to account for long-range ion-ion interactions and short-range (local) interactions between all true species in the liquid phase, while vapor-phase fugacity coefficients were represented with the PRSV equation of state.

The equilibrium distribution of liquid-phase species was determined by a Gibbs free energy minimization technique in which the values of the free energy are constrained by the elemental abundance equations. The minimum in the Gibbs free energy was found by the method of Lagrange multipliers. Due to the non-linearity in mole numbers, the necessary conditions for a minimum in the free energy were satisfied by solving iteratively a linearized set of the necessary conditions. Overall, this procedure converged in a few iterations without any difficult for all systems so far studied.

Binary interaction parameters of the Electrolyte-NRTL equation and carbamate stability constants were fitted on binary system (MEA-H_2O and MDEA-H_2O) and ternary system (H_2S-MEA-H_2O, CO_2-MEA-H_2O, H_2S-DEA-H_2O, CO_2-DEA-H_2O, H_2S-DGA-H_2O, CO_2-DGA-H_2O, H_2S-DMEA-H_2O and CO_2-MDEA-H_2O) vapor-liquid equilibrium data in temperature range from 25 to 120°C.

Ternary vapor-liquid equilibrium data used to estimate the model parameters ranged in alkanolamine concentration from 1 to 5 M, in liquid phase acid gas loading from 0 to 1.5 moles of acid gas per mole of amine, and in acid gas partial pressure from 0.1 to about 100 bar.

Estimates of equilibrium partial pressures and liquid phase apparent mole fractions for H_2S and CO_2, were found, in general, to be in good agreement with ternary (H_2S-alkanolamine-H_2O and CO_2-alkanolamine-H_2O) experimental data for aqueous solutions of MEA, DEA, DGA, and MDEA. That is, the model correctly represents the solubility of H_2S and CO_2 in aqueous solutions of these amines as exhibited by σ_P in Tables V and VII, and Figs. 3 and 4.

In addition, predictions performed for CO_2-alkanolamine-H_2O and H_2S-alkanolamine-H_2O systems show that the developed model can be used for interpolations of the data or extrapolations in regions beyond where measurements have been made.

Finally, an extension of the model has been made to represent H_2S and CO_2 solubility in aqueous solutions of mixed amines data. Results obtained with the fitted parameters for various mixed amines systems will be reported in a forthcoming paper.

Appendix A

Activity coefficients for the Electrolyte-NRTL equation

Pitzer-Debye -Hückel contribution :

Solvent

$$\ln \gamma^*_{s,\mathrm{PDH}} = 2\left(\frac{1000}{M_m}\right)^{\frac{1}{2}} A_\phi \frac{I_x^{3/2}}{(1+\rho I_x^{1/2})}. \qquad \text{(A-1)}$$

Ionic species

$$\ln \gamma_{i,\mathrm{PDH}} = -\left(\frac{1000}{M_m}\right)^{1/2} A_\phi \left[\frac{2z_i^2}{\rho}\ln(1+\rho I_x^{1/2}) + \frac{z_i^2 I_x^{1/2} - 2I_x^{3/2}}{1+\rho I_x^{3/2}}\right]. \qquad \text{(A-2)}$$

Born contribution:

Ionic species

$$\ln \gamma^\infty_{i,\mathrm{PDH}} = -\left(\frac{e^2}{2kT}\right)\left(\frac{z_i^2}{r_i}\right)\left(\frac{1}{D_m} - \frac{1}{D_w}\right). \qquad \text{(A-3)}$$

NRTL contribution:

Molecular species

$$\ln \gamma_{m,\mathrm{NRTL}} = \frac{\sum_j X_j G_{jm}\tau_{jm}}{\sum_k X_k G_{km}} + \sum_{m'} \frac{X_{m'} G_{mm'}}{\sum_k X_k G_{km'}}\left(\tau_{mm'} - \frac{\sum_k X_k G_{km'}\tau_{km'}}{\sum_k X_k G_{km'}}\right) + \sum_c \sum_{a'} \frac{X_{a'}}{\sum_{a''} X_{a''}}\left(\frac{X_c G_{mc,a'c}}{\sum_k X_k G_{kc,a'c}}\right)\left(\tau_{mc,a'c} - \frac{\sum_k X_k G_{kc,a'c}\tau_{kc,a'c}}{\sum_k X_k G_{kc,a'c}}\right) + \sum_a \sum_{c'} \frac{X_{c'}}{\sum_{c''} X_{c''}}\left(\frac{X_a G_{ma,c'a}}{\sum_k X_k G_{ka,c'a}}\right)\left(\tau_{ma,c'a} - \frac{\sum_k X_k G_{ka,c'a}\tau_{ka,c'a}}{\sum_k X_k G_{ka,c'a}}\right). \qquad \text{(A-4)}$$

$$\ln \gamma^\infty_{m,\mathrm{NRTL}} = \tau_{mw} + G_{mw}\tau_{mw} \qquad \text{(A-5)}$$

Cations

$$\frac{1}{Z_c}\ln\gamma_{c,\mathrm{NRTL}} = \sum_{a'}\frac{X_{a'}}{\sum_{a''}X_{a''}}\left(\frac{\sum_k X_k G_{kc,a'c}\tau_{kc,a'c}}{\sum_k X_k G_{kc,a'c}}\right) + \sum_m \frac{X_m G_{km}}{\sum_k X_k G_{km}}\left(\tau_{cm} - \frac{\sum_k X_k G_{km}\tau_{km}}{\sum_k X_k G_{km}}\right) + \sum_a\sum_{c'}\frac{X_{c'}}{\sum_{c''}X_{c''}}\left(\frac{X_a G_{ca,c'a}}{\sum_k X_k G_{ca,c'a}}\right)\left(\tau_{ca,c'a} - \frac{\sum_k X_k G_{ka,c'a}\tau_{ka,c'a}}{\sum_k X_k G_{ka,c'a}}\right). \quad \text{(A-6)}$$

$$\ln\gamma^{\infty}_{c,\mathrm{NRTL}} = Z_c\left(G_{cw}\tau_{cw} + \frac{\sum_{a'}X_{a'}\tau_{wc,a'c}}{\sum_{a''}X_{a''}}\right) \quad \text{(A-7)}$$

Anions

$$\frac{1}{Z_a}\ln\gamma_{a,\mathrm{NRTL}} = \sum_{c'}\frac{X_{c'}}{\sum_{c''}X_{c''}}\left(\frac{\sum_k X_k G_{ka,c'a}\tau_{ka,c'a}}{\sum_k X_k G_{ka,c'a}}\right) + \sum_m \frac{X_m G_{km}}{\sum_k X_k G_{km}}\left(\tau_{am} - \frac{\sum_k X_k G_{km}\tau_{km}}{\sum_k X_k G_{km}}\right) + \sum_c\sum_{a'}\frac{X_{a'}}{\sum_{a''}X_{a''}}\left(\frac{X_c G_{ac,a'c}}{\sum_k X_k G_{ac,a'c}}\right)\left(\tau_{ac,a'c} - \frac{\sum_k X_k G_{kc,a'c}\tau_{kc,a'c}}{\sum_k X_k G_{kc,a'c}}\right). \quad \text{(A-8)}$$

$$\ln\gamma^{\infty}_{a,\mathrm{NRTL}} = Z_a\left(G_{aw}\tau_{aw} + \frac{\sum_{c'}X_{c'}\tau_{wa,c'a}}{\sum_{c''}X_{c''}}\right) \quad \text{(A-9)}$$

Activity coefficients given by Eqs. (A-4), (A-6) and (A-8) are symmetrically normalized. Therefore, to obtain the unsymmetrically normalized activity coefficients for which the solute (molecular or ionic) reference state is the ideal infinitely dilute aqueous solution, Eqs. (A-5), (A-7) and (A-9) must be subtracted from the corresponding expressions for the symmetrically normalized activity coefficients.

---

*. Author to whom correspondence should be addressed

1. R.N. Maddox, " Gas and Liquid Sweetening ", *Gas Conditioning and Processing*, Vol. 4. 3rd edn., (Campbell Petroleum Series, Norman, OK, 1985).
2. A.L. Kohl and F.C. Riesenfeld, *Gas Purification*, 4th edn., (Gulf Publishing Co., Houston, TX, 1985).
3. T. Chakravarty, U.K. Phukan, and R.H. Weiland, *Chem. Eng. Progr.* **81** (1985) 32.
4. F. Murrieta-Guevara and A. Trejo, *J. Chem. Eng. Data* **29** (1984) 456.
5. F. Murrieta-Guevara, A. Romero-Martínez, and A. Trejo, *Fluid Phase Equilibria* **44** (1988) 105.
6. F. Murrieta-Guevara, E. Rebolledo-Libreros, and A. Trejo, *Fluid Phase Equilibria* **53** (1989) 1.
7. F. Murrieta-Guevara, E. Rebolledo-Libreros, and A. Trejo, *J. Chem. Eng. Data* **37** (1992) 4.
8. F. Murrieta-Guevara, E. Rebolledo-Libreros, and A. Trejo, *Fluid Phase Equilibria* **73** (1992) 167.
9. F. Murrieta-Guevara, E. Rebolledo-Libreros, and A. Trejo, *Fluid Phase Equilibria* **86** (1993) 225.
10. F. Murrieta-Guevara, E. Rebolledo-Libreros, and A. Trejo, *Fluid Phase Equilibria* **95** (1994) 163.
11. R.D. Deshmukh and A.E. Mather, *Chem. Eng. Sci.* **36** (1981) 355.
12. C.-C. Chen and L.B. Evans, *AIChE J.* **32** (1986) 444.
13. T. Chakravarty, Doctoral Dissertation, Clarkson College, Postdam, NY (1985).
14. D.M. Austgen, G.T. Rochelle, X. Peng, and C.-C. Chen, *Ind. Eng. Chem.Res.* **28** (1989) 1060.
15. D.M. Austgen, G.T. Rochelle, and C.-C. Chen, *Ind. Eng. Chem. Res.* **30** (1991) 543.

16. T.J. Edwards, G Maurer, J. Newman, and J.M. Prausnitz, *AIChE J.* **24** (1978) 966.

17. S.W. Brelvi and J.P. O'Connell, *AIChE J.* **18** (1972) 1239.

18. C.F. Spencer and R.P. Danner, *J. Chem. Eng. Data* **17** (1976) 236.

19. J. Keenan and F.G. Keyes, *Thermodynamic Properties of Steam*, (John Wiley & Sons, NY, 1950).

20. D.-Y. Peng and D.B. Robinson, *Ind. Eng. Chem. Fundam.* **15** (1976) 59.

21. R. Stryjek and J.H. Vera, *Can. J. Chem. Eng.* **64** (1986) 323.

22. K.S. Pitzer, *J. Amer. Chem. Soc.* **102** (1980) 2902.

23. R.A. Robinson and R.H. Stokes, *Electrolyte Solutions.* 2nd. edn., (Butterworth & Co., London, 1970).

24. H.C. Helgeson and D.H. Kirkham, *Amer. J. Sci.* **274** (1974) 1089.

25. J.M. Prausnitz and P.L. Chueh, *Computer Calculations for High-Pressure Vapor-Liquid Equilibria*, (Prentice-Hall, Inc., Englewood Cliffs, NJ, 1968).

26. H. Renon and J.M. Prausnitz, *AIChE J.* **14** (1968) 135.

27. W.R. Smith and R.W. Missen, *Chemical Reaction Equilibrium Analysis:Theory and Algorithms*, (John Wiley & Sons, NY, 1982).

28. B. Mock, L.H. Evans, and C.-C. Chen, *AIChE J.* **32** (1986) 1655.

29. J.A. Nelder and R. Mead, *The Computer J.* **7**(1965)308.

30. H. Chang, M. Posey, and G.T. Rochelle, *Ind. Eng. Chem. Res.* **32** (1993) 2324.

31. J.C. Dingman, J.L. Jackson, T.F. Moore, and J.A. Branson, Paper presented at the 62nd Annual Gas Processors Association Convention, San Francisco, CA, (1983).

32. T.E. Daubert and R.P. Danner, *Data Compilation Tables of Properties of Pure Compounds, Design Institute for Physical Property Data*, (American Institute of Chemical Engineers, NY, 1985).

33. T.E. Daubert and G. Hutchinson, *AIChE Symp. Ser.*, **86** No.279, NY, (1990).

34. D.M. Austgen, Doctoral Dissertation, University of Texas at Austin, Austin, TX, (1989).

35. R.C. Reid, J.M. Prausnitz, and B.E. Poling, *The Properties of Gases and Liquids*, 4th edn., (McGraw-Hill Book Co., NY, 1987).

36. J.J. Carroll, F.-Y. Jou, A.E. Mather, and F.D. Otto, *AIChE J.* **38** (1992) 511.

37. J.I. Lee, F.D. Otto, and A.E. Mather, *J. Appl. Chem. Biotechnol.* **26** (1976) 541.

38. E.E. Isaacs, F.D. Otto, and A.E. Mather, *J. Chem. Eng. Data* **25** (1980) 118.

39. J.D. Lawson, and A.W. Garst, *J. Chem. Eng. Data* **21** (1976) 20.

40. J.H. Jones, H.R. Froning, and E.E. Claytor, *J. Chem. Eng. Data* **4** (1959) 85.

41. H.G. Muhlbauer and P.R. Monaghan, *Oil & Gas J.* **55** (1957) 139.

42. J.I. Lee, F.D. Otto, and A. E. Mather, *Can. J. Chem. Eng.* **52** (1974) 803.

43. J.I Lee, F.D. Otto, and A.E. Mather, *J. Chem. Eng. Data* **21** (1976) 207.

44. J.I. Lee, F.D. Otto, and A.E. Mather, *J. Chem. Eng. Data* **17** (1972) 465.

45. D. Lal, F.D. Otto, and A.E. Mather, *Can. J. Chem. Eng.* **63** (1985) 681.

46. J.I. Lee, F.D. Otto, and A.E. Mather, *J. Chem. Eng. Data* **18** (1973) 71.

47. J.I. Lee, F.D. Otto, and A.E. Mather, *J. Chem. Eng. Data* **18** (1973) 420.

48. K. Atwood, M. R. Arnold, and R.C. Kindrick, *Ind. Eng. Chem.* **49** (1957) 1439.

49. F.Y. Jou, A.E. Mather, and F.D. Otto, *Ind. Eng. Chem. Process Des. Dev.* **21** (1982) 539.

50. F.Y. Jou, F.D. Otto, and A.E. Mather, Paper No. 140b presented at the Annual Meeting of the AIChE, Miami Beach, FL (1986)

51. A.M. Bhairi, Doctoral Dissertation, Oklahoma State University, OK (1984).

52. N.B. Matin, S.M. Danov, and R.V. Efremov, *Tr. Khim. Teknol.* **2** (1969) 7.